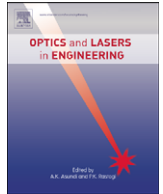


This article appeared in a journal published by Elsevier. The attached copy is furnished to the author for internal non-commercial research and education use, including for instruction at the authors institution and sharing with colleagues.

Other uses, including reproduction and distribution, or selling or licensing copies, or posting to personal, institutional or third party websites are prohibited.

In most cases authors are permitted to post their version of the article (e.g. in Word or Tex form) to their personal website or institutional repository. Authors requiring further information regarding Elsevier's archiving and manuscript policies are encouraged to visit:

<http://www.elsevier.com/copyright>



Digital sinusoidal fringe pattern generation: Defocusing binary patterns VS focusing sinusoidal patterns

Shuangyan Lei, Song Zhang *

Mechanical Engineering Department, Iowa State University, Ames, IA 50011, USA

ARTICLE INFO

Article history:

Received 23 October 2009

Received in revised form

3 December 2009

Accepted 7 December 2009

Available online 4 January 2010

Keywords:

3-D shape measurement

Optical metrology

Digital fringe projection

Fringe analysis

Optical metrology

Defocusing

ABSTRACT

There are two approaches to generate sinusoidal fringe patterns with a digital-light-processing (DLP) projector: defocusing binary patterns (DBP), and focusing sinusoidal patterns (FSP). This paper will compare the potential errors for both methods induced by the following factors: (1) degree of defocusing, (2) exposure time, (3) synchronization, and (4) projector's nonlinear gamma. Experiments show that in most scenarios, the error for the DBP method is smaller than that of the FSP method. Therefore, generating a sinusoidal fringe image using a DBP method seems to be appealing.

© 2009 Elsevier Ltd. All rights reserved.

1. Introduction

3-D shape measurement using a digital-light-processing (DLP) projector becomes increasingly popular over the past few years [1]. Among the existing 3-D shape measurement techniques, fringe projection technique is one of the most widely adopted ones. However, there are some practical issues to be considered for high quality measurement, as thoroughly discussed by Wang et al. [2].

Conventionally, sinusoidal fringe patterns are usually supplied to an focused projector to do 3-D shape measurement, which is called focusing-sinusoidal-patterns (FSP) method. Although widely adopted, they have some of major drawbacks: (1) It is very sensitive to nonlinear gamma of the projector. The phase error is very larger if no gamma calibration is adopted; (2) The camera and the projector must be precisely synchronized for high-quality measurement. This is mostly because the nature of the DLP technology that generates grayscale images by time integration; and (3) the exposure time of the camera must be precisely controlled, especially when a short exposure time is used.

To avoid these problems, one approach is to use the DLP Discovery platform developed by Texas Instruments (TI). With DLP Discovery board, high-speed, highly linear sinusoidal fringe patterns can be generated, and the synchronization between the camera and the projector can be precisely controlled [3,4]. However, comparing with a commercial DLP projector, the DLP Discovery platform is much more expensive. Therefore, studying

how to use a commercial projector to realize high-quality measurement is highly needed.

Our recent study indicated that it is feasible to generate high-quality sinusoidal fringe patterns by properly defocusing binary structured patterns [5]. Therefore, instead of sending sinusoidal fringe images to an focused projector, sinusoidal fringe patterns can be generated by defocusing binary patterns (DBP).

In this research, we will demonstrate that for the DBP method: (1) There is no need to calibrate the nonlinear gamma of the projector because only two intensity levels are used; (2) It is very easy to generate sinusoidal fringe patterns because no complicated algorithms are necessary; (3) There is no need to precisely synchronize the projector with the camera; and (4) The measurement is less sensitive to exposure time used. Therefore, the DBP method is advantageous for 3-D shape measurement using a commercial DLP projector.

Our first study focuses on understanding how the degree of defocusing affects the measurement error. We simulate the defocusing effect by applying a Gaussian smoothing filter, different degree of defocusing is realized by using different size of filters. A three-step phase-shifting algorithm is adopted to compute the phase, whose error is analyzed at different level of defocusing. The degree of defocusing is realized by adjusting the focal length of the projector while keeping the physical relationship between the projector and the object constant. Both simulation and experiment showed that the phase error caused by defocusing does not change significantly over a larger range.

For a DLP projector, the grayscale values of an image are generated digitally by time integration [6]. To capture correct grayscale images, the camera must exposure the whole projection

* Corresponding author. Tel.: +1 515 294 0723; fax: +1 515 294 3261.
E-mail address: song@iastate.edu (S. Zhang).

time. This means that (1) the synchronization between the projector and the camera is vital and (2) the exposure time of the camera must be precisely controlled. On the contrast, the DBP technique only uses two grayscale values (0 and 255 s), because these requirements are not very strict. This study will also compares the influence of these two factors.

As indicated in the previous studies, for high-quality measurement, the projector's nonlinear gamma must be corrected or compensated where FSP method used [2], while it is not necessary for the DBP method because only two intensity values are used. Experiments will also be conducted to find the difference.

Section 2 presents the principle of a three-step phase-shifting algorithm. Section 3 shows the simulation result for generating sinusoidal fringe patterns with the DBP method. Section 4 compares the phase errors under various conditions. Section 5 discusses the advantages and shortcomings of the DBP method in comparison with the FSP method, and Section 6 summarizes this paper.

2. Three-step phase-shifting algorithm

Optical metrology using fringe analysis is widely used in numerous applications because of its measurement accuracy and non-contact surface measurement nature. In order to perform a measurement, the phase needs to be retrieved from the fringe images. The phase can be obtained through a single fringe image [7] or dual fringe images by a Fourier method [8], or multiple fringe images with different spatial phase shift through a phase-shifting method [9]. While many phase-shifting methods have been developed including three-step, four-step, and double three-step algorithms; the differences between them relates to the number of fringe images recorded, the phase shift between these fringe images, and the susceptibility of the algorithm to errors in the phase shift, environmental noise such as vibration and turbulence as well as nonlinearities of the detector when recording the intensities [10]. Among these algorithms, the three-step phase-shifting algorithm utilizes the minimum number of fringe images, thus achieve the fastest measurement speed. Even though other algorithms can be used to perform the analysis, a three-step phase shifting algorithm with a phase shift of $2\pi/3$ is used for its simplicity. The intensities of three phase-shifted fringe images are

$$I_1(x, y) = I'(x, y) + I''(x, y)\cos[\varphi(x, y) - 2\pi/3], \quad (1)$$

$$I_2(x, y) = I'(x, y) + I''(x, y)\cos[\varphi(x, y)], \quad (2)$$

$$I_3(x, y) = I'(x, y) + I''(x, y)\cos[\varphi(x, y) + 2\pi/3]. \quad (3)$$

Here $I'(x, y)$ is the average intensity, $I''(x, y)$ the intensity modulation, and $\varphi(x, y)$, the phase to be solved for. Solving Eqs. (1)–(3) simultaneously, we obtain the phase

$$\phi(x, y) = \tan^{-1} \left[\frac{\sqrt{3}(I_1 - I_3)}{2I_2 - I_1 - I_3} \right]. \quad (4)$$

This equation indicates that the phase value obtained ranges from $-\pi$ to $+\pi$. To obtain a continuous phase map, a phase unwrapping algorithm is applied to detect the 2π discontinuities and remove them by adding or subtracting multiples of 2π [11].

3. Simulation

The defocusing effect can be approximated as a Gaussian smoothing filter. The degree of defocusing can be controlled by applying different size of filters or by applying the same

size of filters at different number of times. The latter approach is adopted in this research. A 2-D Gaussian filter is usually defined as

$$G(x, y) = \frac{1}{2\pi\sigma^2} e^{-(x-\bar{x})^2 + (y-\bar{y})^2 / 2\sigma^2}. \quad (5)$$

Here σ is the standard deviation and \bar{x} , \bar{y} are the mean of x and y , respectively.

In this simulation, the structured stripes are either vertical or horizontal, because only one cross section perpendicular to the fringe stripes needs to be considered, thus the problem is reduced to a 1-D problem. A 1-D Gaussian filter is defined as

$$G(x) = \frac{1}{\sqrt{2\pi}\sigma} e^{-(x-\bar{x})^2 / 2\sigma^2}. \quad (6)$$

We started with the cross section of a binary structured pattern (square wave) as shown in Fig. 1(a). The binary pattern is then smoothed with a Gaussian filter with nine pixels and standard deviation of 4.5 pixels, the result is shown in Fig. 1(b). The sharp edges start softening, and the square wave becomes trapezoidal in shape. If the same filter is applied again, the waveform is close to be sinusoidal, but the top and bottom remain flat, as shown in Fig. 1(c). Figs. 1(d–f) show the results when the filter is applied the third, fourth, and fifth times. It clearly shows that the wave becomes more and more sinusoidal. One should notice that the amplitude of the sinusoidal wave reduces as the degree of defocusing increases. This indicates that the fringe contrast drops accordingly. For a real measurement system, this may result in larger error because the quantization error of a digital camera is larger. For the simulation, a floating point is used, because the quantization error is not very significant.

The phase shift is introduced by spatially moving the binary patterns. For example, a $2\pi/3$ phase shift can be realized by moving $1/3$ period of the binary pattern. Once three phase-shifted fringe patterns are generated, Eq. (4) can be applied to compute the phase. The wrapped phase is then unwrapped to remove 2π discontinuities, and the slope of the unwrapped phase is removed to better show the phase errors. Fig. 2 shows the corresponding phase for the smoothed fringe images shown in Fig. 1. For a square wave, the phase error is very large, root mean square (RMS) 0.3018 rad or $0.3018/(2\pi) \times 100\% = 4.8\%$, as shown in Fig. 2(a). On the contrast, if the profile of the fringe becomes seemingly sinusoidal, such as Figs. 2(d–f), the phase errors are always $< 0.06\%$, which can be negligible. Therefore, once the binary structured patterns are defocused to be sinusoidal, further defocusing will not significantly increase the phase error. However, in a real 3-D shape measurement system, if the degree of defocusing is too low, fringe contrast will be very low. Even though some fringe enhancement techniques can be used [12], the random noise will bring significant error into the phase. It should be noted that the phase error shown in this simulation appears to be periodical, which might be caused by the finite filter size used. This type of periodical phase error might not appear in real measurement system because the lens defocusing acts as an analog device and the problem related to discrete filtering is not there.

4. Experiments

4.1. Test system

We developed a hardware system to perform various tests. The system includes The Imaging Source Digital USB CCD camera (DMK 21BU04) with Computar M0814-MP (F1.4) lens, and the

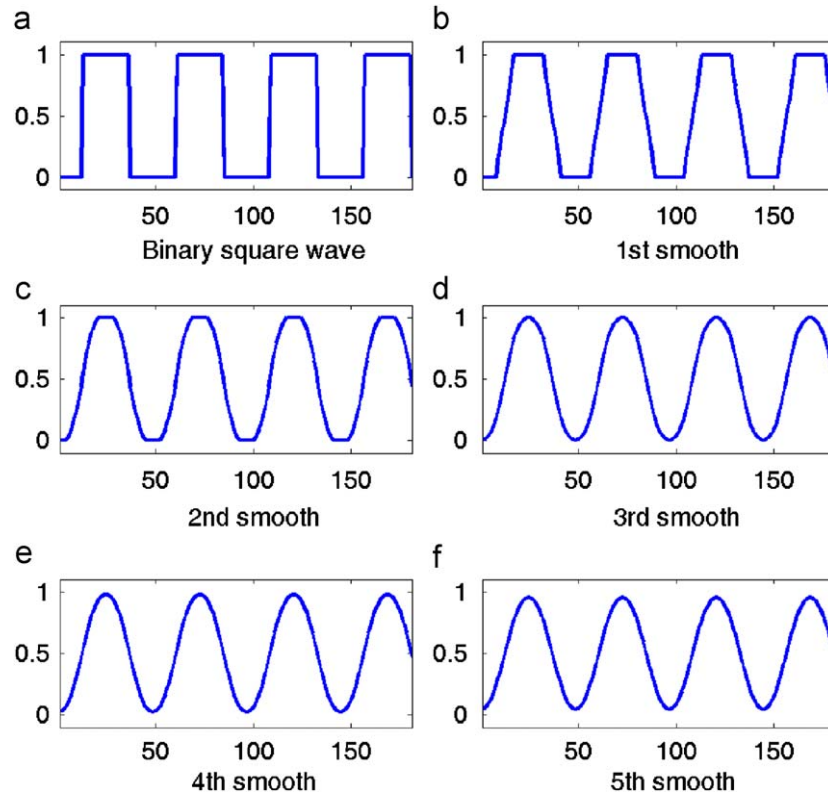


Fig. 1. Schematic diagram of the hybrid algorithm.

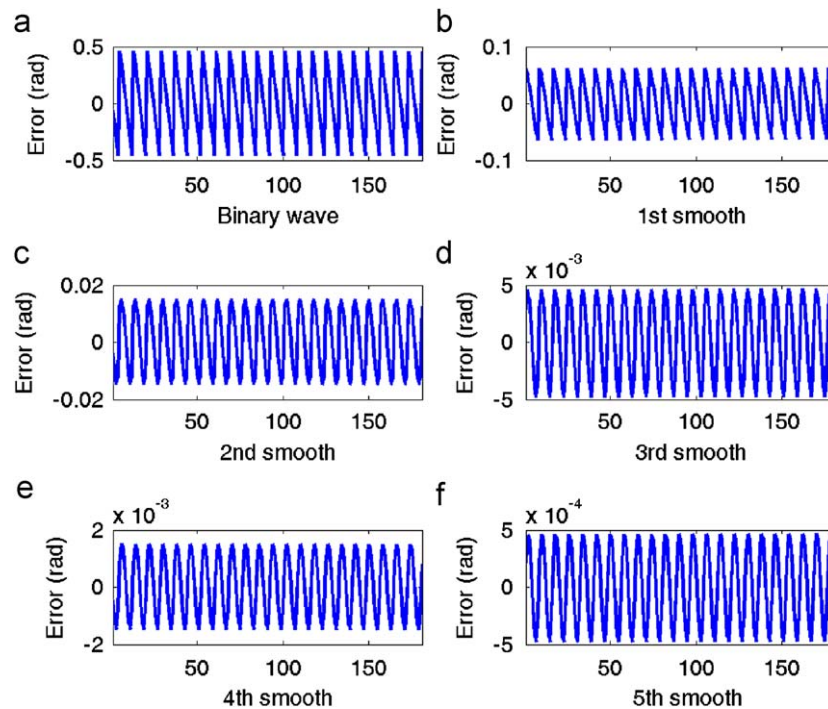


Fig. 2. RMS phase error for different smoothing level from (a–f) are 0.3018, 0.0442, 0.0115, 0.0035, 0.0011, 0.0003 rad, respectively.

Dell projector (M109S). The camera resolution is 640×480 , with a maximum frame rate of 60 frames/s. The pixel size of the camera sensor is $5.6 \times 5.6 \mu\text{m}^2$. The projector has a resolution of 858×600 with a lens of F/2.0, $f = 16.67 \text{ mm}$. The projection distance is 23.6–94.5 in. The DMD used in this projector is 0.45-inch Type Y chip. This projector uses Texas

Instrument BrilliantColorTM technology to enhance the brightness and color gamut [13]. Instead of using red, green, blue (RGB) three colors, the BrilliantColorTM technology uses five colors including yellow and cyan to use coupling spectra between RG and GB. To simplify the test, only green channel is used for all tests.

To understand how the projector projects images, a pure green RGB = (0, 255, 0) image is sent to the projector and a photodiode is used to monitor the output light. Fig. 3 shows the signal output displayed on an oscilloscope. Here channel 1 of the oscilloscope shows the detected signal and channel 2 shows VSync of the video graphics array (VGA) signal connected with the projector. Because the projector is synchronized with this VSync signal, its projection cycle is 1/60 s. This figure shows that five pulses are roughly equally distributed within the projection period (1/60 s), with one duration time of approximately 1.67 ms.

4.2. Defocusing degree

A uniform flat surface is imaged to find out the phase error at various defocusing degrees. During the experiments, the camera is synchronized with VSync of the projector, the exposure time is set to be one projection cycle (i.e., 16.67 ms), and the defocusing is realized by adjusting the projector's focal distance. Figs. 4(a–f) show the

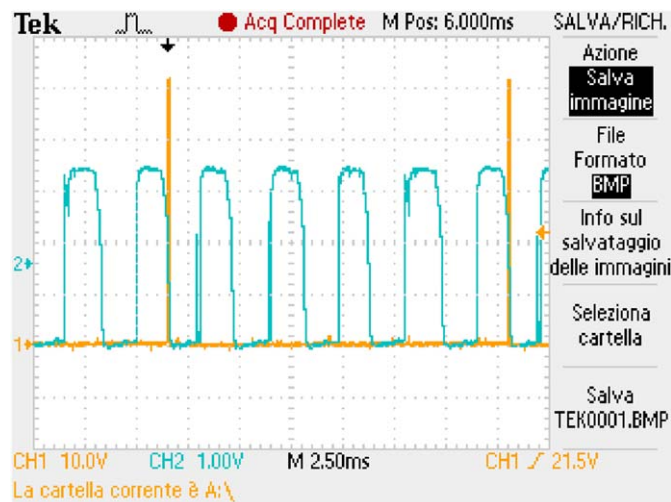


Fig. 3. Projector timing signal with a pure green input. (For interpretation of the references to colour in this figure legend, the reader is referred to web version of this article.)

fringe images when a binary structured pattern is supplies to the projector, and Figs. 4(g–l) show the corresponding images when the projector is fed with sinusoidal ones. At level 1, both the projector and the camera are in focus, therefore the fringe patterns have very obvious binary structures for the DBP method, as shown in Fig. 4(a). With the increase of the defocusing degree, the binary structures are less and less clear, and they become more and more sinusoidal. However, if the defocusing degree is too much, sinusoidal structure becomes obscure, as indicated in Fig. 4(f).

As a comparison, if the projector is supplied with a sinusoidal pattern, the fringe image has very high contrast when the projector is in focus, as shown in Fig. 4(g). However, when the projector is defocused, the fringe contrast is lower than its DBP counterpart. Therefore, when the projector is defocused to a degree, the fringe quality for the DBP method is better than that for the FSP method.

If three phase-shifted fringe images are acquired, the phase can be recovered using Eq. (4). The phase is unwrapped to remove 2π discontinuities, and its slope is removed to better show the phase errors. It should be noted that for the FSP method, a nonlinear gamma calibration method introduced in Ref. [14] is adopted to ensure the projector project ideal sinusoidal fringe images.

Fig. 5 shows the phase errors when the DBP is used. If both the projector and the camera are in focus, the phase error is very large. With the degree of defocusing increases, better and better sinusoidal fringes will be generated for the DBP method, and the phase error becomes smaller and smaller. However, when the degree of defocusing is too much, and the phase error increases again because the fringe contrast decreases. This experiment indicates that there is a large range of defocusing when the phase error is relatively small. It also indicates that it is not necessary to control the degree of defocusing precisely to perform high quality measurement, therefore, the DBP method can be used for general 3-D shape measurement with a large depth range.

Fig. 6 shows the results if the FSP method is used. When the projector is in focus, no obvious periodical error appears. This means that the projector's gamma correction is performed reasonably well. However, when the projector starts defocusing, periodical errors appears. The error seems to be dominated by single-frequency component. The single frequency error is usually caused by the imbalance of three fringe images. As a comparison,

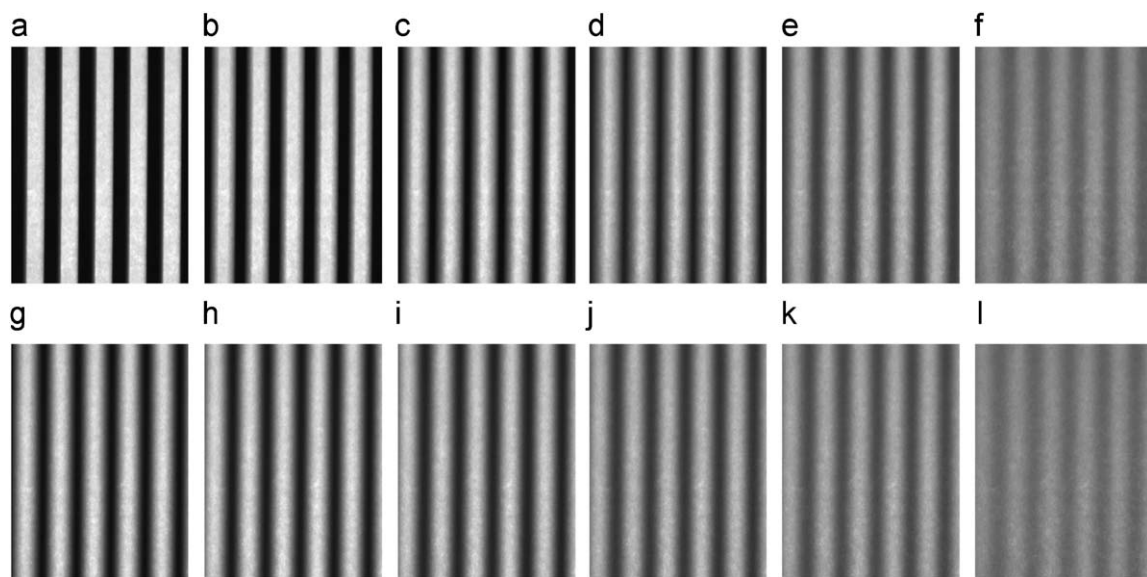


Fig. 4. Fringe images for DBP and FSP methods at different defocusing levels. Level 1 is in focus and level 6 is severely defocused. (a–f) show the fringe images generated by the DBP method with defocusing levels from 1 to 6, and (g)–(l) show the fringe images generated by FSP method with defocusing levels from 1 to 6.

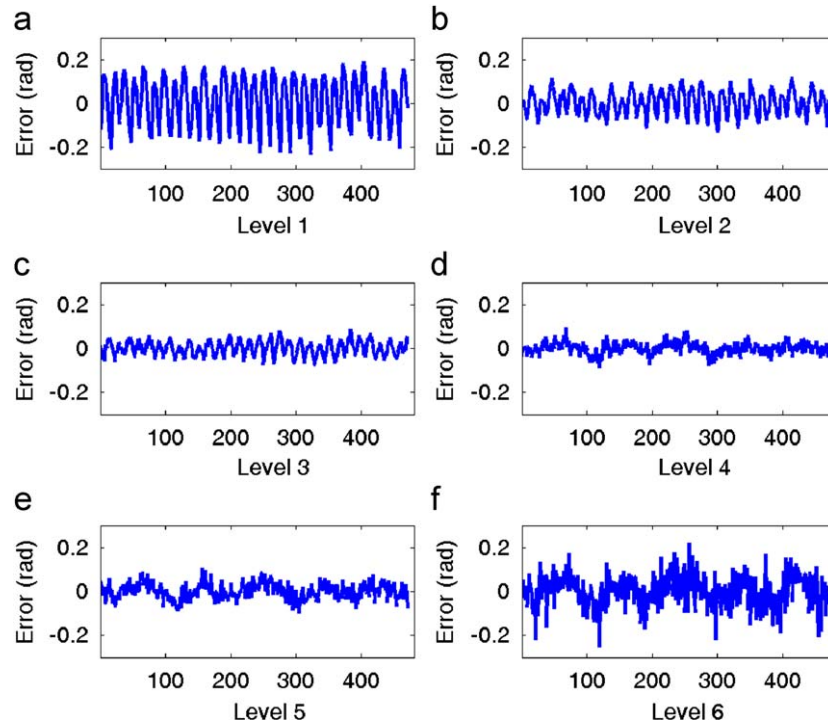


Fig. 5. Phase error for different defocusing level of fringe images is shown in Fig. 4 first row. The RMS errors in (a–f) are 0.121, 0.058, 0.017, 0.022, 0.030, 0.071 rad, respectively.

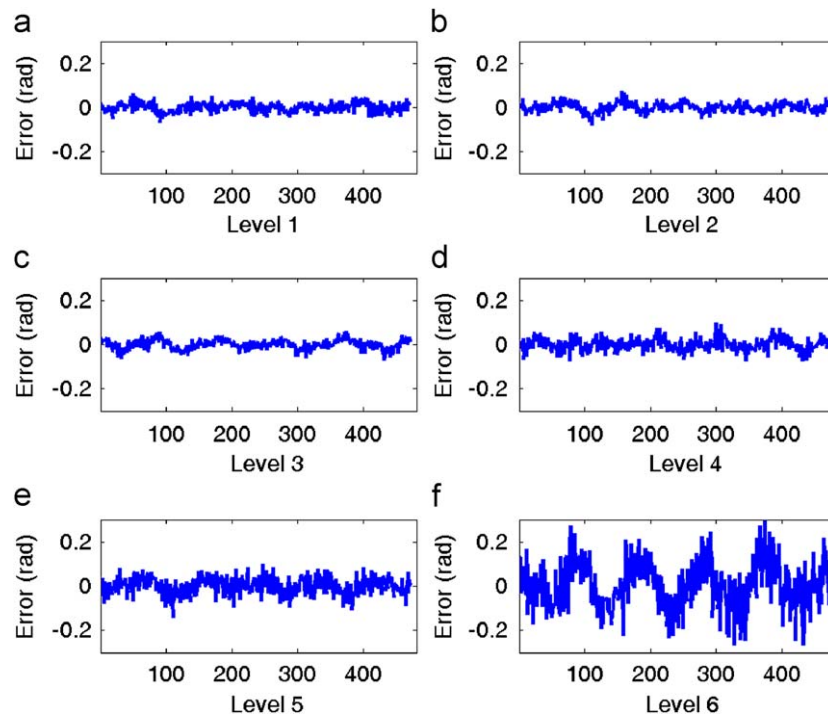


Fig. 6. Phase error for different defocusing level of fringe images is shown in Fig. 4 second row. The RMS error in (a–f) are 0.017, 0.020, 0.023, 0.029, 0.035, 0.079 rad, respectively.

the phase error generated by the DBP method is smaller. One of the reasons behind might be the gamma of the projector is a complicated curve, thus is not easy to be precisely represented with a mathematical equation through calibration. Another reason could be the precision of the synchronization between the projector and the camera, which will be investigated in Section 4.4.

Fig. 7 compares the phase errors introduced by these two methods under different degree of defocusing. This figure indicates that when the projector is in focus, the phase error for the DBP method is larger. It also indicates that when the projector is defocused to a degree, the phase error induced by the DBP method is actually smaller than that produced by the FSP method. It is interesting to notice that under their own best condition, i.e.,

the projector is in focus for the FSP method, and the projector is properly defocused for the DBP method, the phase error is very close. This experiment indicates that it is possible to generate ideal sinusoidal fringe patterns by defocusing binary patterns.

4.3. Exposure time

To evaluate how the camera's exposure time influences the measurement, various exposure time is tested and the phase errors are calculated accordingly. The camera is synchronized with the projector's VSync signal when the projector starts a new projection cycle. The exposure time is chosen so that sometimes it captures the projection pulse partially and sometimes it capture completely. The projector uses the BrilliantColor™ technology, for green channel, five pulses are generated within one projection cycle, as shown in Fig. 3. Fig. 8 illustrates how the camera exposures. The camera always starts its exposure when the VSync signal comes, and stops at different timing. The 10 different exposures (2.50, 4.17, 5.83, 7.50, 9.17, 10.83, 12.50, 14.17, 15.80, 16.67 ms) are used for data acquisition. For this experiment, only green channel is used to simplify the experiment. Because the exposure time of the camera varies, aperture is adjusted accordingly to acquire high quality fringe images. It should be noted that the projector is properly defocused so that high-quality sinusoidal fringe patterns are generated.

For the same exposure condition, we also tested the FSP method. For this method, the projector is in focus, and its gamma curve is calibrated and corrected. Fig. 9(a) shows one of the fringe images when the exposure time is set to be 2.50 ms. The nonsinusoidal waveforms are clearly shown in this image because the camera does not capture the full projection period.

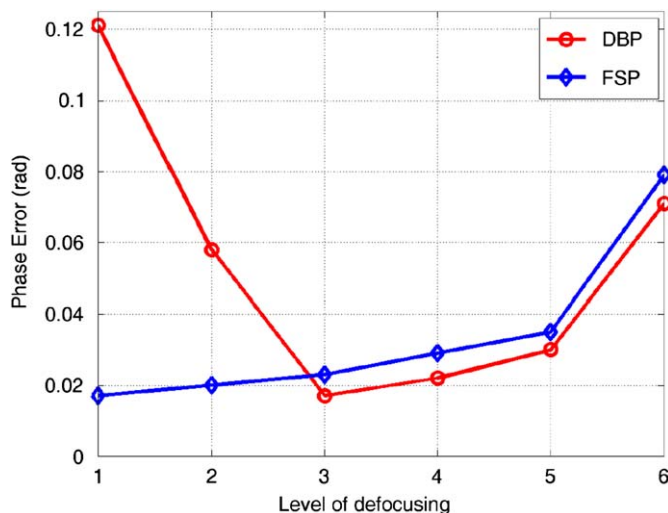


Fig. 7. Phase error for different smoothing levels of fringe images is shown in Figs. 5 and 6.

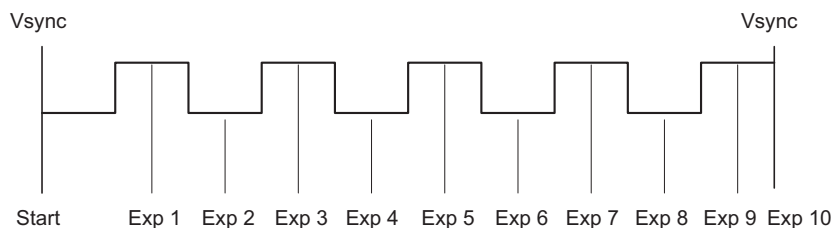


Fig. 8. Timing of the camera exposures. All exposure starts when the VSync signal comes, and stops at different timing. Exp 1, 2, ..., and 10 use exposure time of 2.50, 4.17, 5.83, 7.50, 9.17, 10.83, 12.50, 14.17, 15.80, 16.67 ms.

For this exposure time, the phase error is very large (RMS 0.152 rad). Fig. 9(c) shows one cross section of phase error for the FSP method. It clearly shows high-frequency periodical error components that are caused by the nonsinusoidal waveform. The nonsinusoidal waveform is a result of the miss-capture of the camera. Because for a DLP projector, the grayscale images are produced using the full projection time, any less exposure can result in an incorrect grayscale image.

As a comparison, for the DBP method, the fringe image captured has high quality, as shown in Fig. 9(b). As a result, the phase error appears random and is much smaller, as indicated in Fig. 9(d).

As the exposure time increases to be 16.67 ms, the camera captures the full projection cycle, thus all the information projected by the projector is captured. The fringe images captured for the FSP method are sinusoidal (Fig. 10(a)) and the phase error appears to be random (Fig. 10(c)). Figs. 10(b and d) show the results for the DBP method; sinusoidal patterns are also very clear and the phase error is still random, even though it is smaller in comparison with that using the exposure time of 2.50 ms.

In general, the phase error is smaller when the whole exposure time is longer due to the averaging effect. However, if the projection is not fully captured and the FSP method is used, the phase error is larger. Fig. 11 shows the phase error VS the exposure time. This experiment clearly shows that for the DBP method, the phase error does not vary significantly with the exposure time, while the FSP method does, especially when the exposure time is short. The phase error is also larger when the camera does not capture the full projection. This experiment shows that if a very short (or arbitrary) exposure time is needed, the DBP method clearly outperforms the FSP method for 3-D shape measurement.

4.4. Synchronization

The synchronization between the projector and the camera plays an important role for high-quality 3-D shape measurement, especially when the exposure time is not long. To test this effect, the external trigger of the camera is disabled, and the fringe images are captured at anytime when the user starts it. In this manner, only the exposure time is defined, while the starting timing is random. Two specific exposure time is tested (3.33 and 6.66 ms). The exposure time is selected so that either one or two pulses of projection will be captured for the projection shown in Fig. 3. In this experiment, for each exposure, the software continuous running with random delays between frames, and 100 frames are captured for each method. Fig. 12 shows the phase errors for all 100 measurements. Figs. 12(a and b) show the results when the exposure time is set as 3.33 ms, and Figs. 12(c and d) show the results when the exposure time is chosen as 6.67 ms. Figs. 12(a and c) are the results for the DBP method and Figs. 12(b and d) are the results for the FSP method. This experiment demonstrated that for the same exposure time, the phase error is much smaller if the DBP method is used. This might be caused by the stability of the projection.

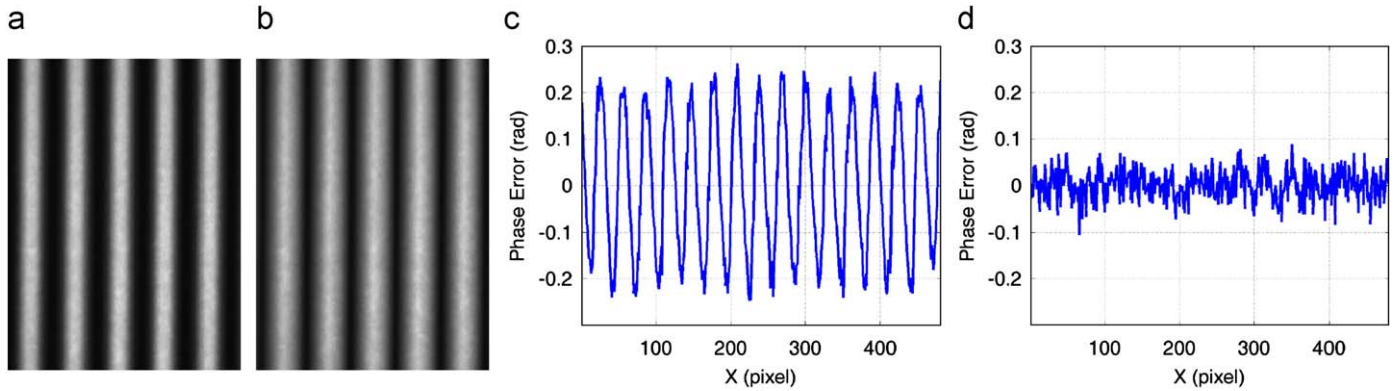


Fig. 9. Fringe images and phase errors if the exposure time is 2.50 ms. (a) Fringe image for FSP method; (b) fringe image for DBP method; (c) one cross section of the phase error map for the FSP method; (d) one cross section of the phase error map for the DBP method.

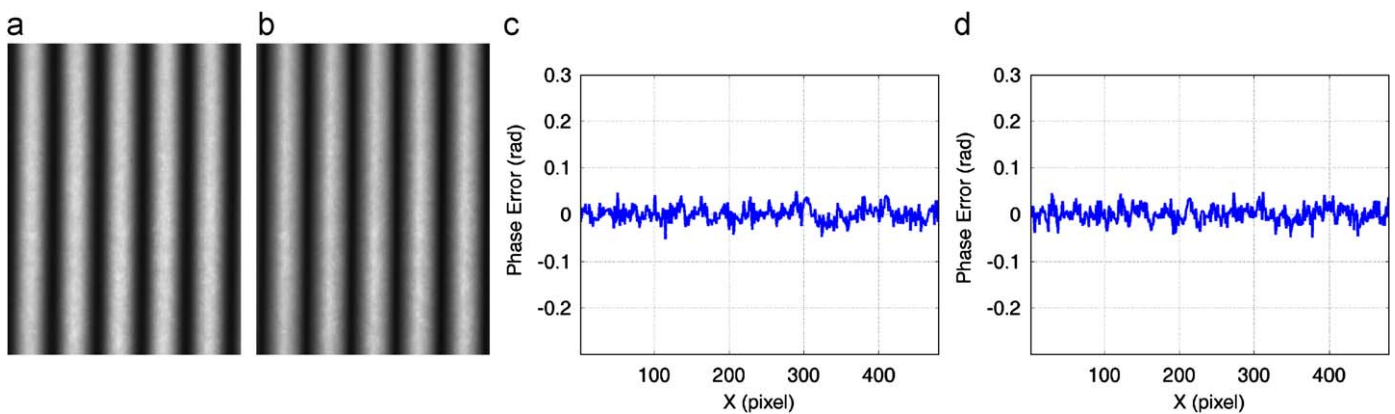


Fig. 10. Fringe and phase error for sinusoidal structured pattern input when exposure time is 16.67 ms. (a) Fringe image for FSP method; (b) fringe image for DBP method; (c) one cross section of the phase error map for the FSP method; (d) one cross section of the phase error map for the DBP method.

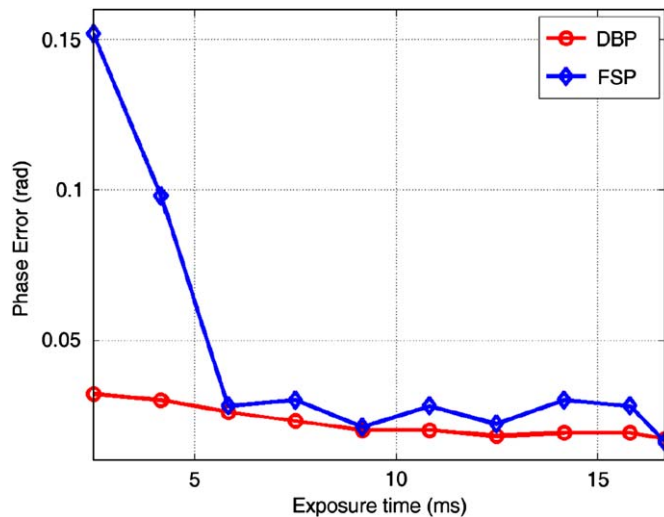


Fig. 11. Fringe images captured with different exposures when the binary structured patterns are defocused to be sinusoidal.

Fig. 13 and the associated video show the comparison between the fringe images captured for the DBP method and the FSP method over time. Where the left is the fringe images when the DBP method is used, while the right shows those when the FSP method is used. It clearly shows that the fringe images for the DBP method only vary intensity over time, but those for the FSP method vary both intensity and the fringe profile. This

experiment clearly shows that the DBP method is less sensitive to the synchronization between the projector and the camera, and outperforms the FSP method when the camera is not precisely synchronized with the projector.

4.5. Projector nonlinear gamma

For the FSP method, the nonlinear gamma corrections of the projector is very important. This is because the projector is purposely designed as a nonlinear device to compensate for human vision. A variety of techniques have been studied including those to actively change the fringe to be projected [14,15], and to passively compensate for the phase error [16–19]. However, for the DBP method, this should not be necessary because only two intensity values are used.

Experiments were performed to verify the performance and to compare the phase errors caused by projector's nonlinear gamma. In this test, exposure time of $t = 16.67$ ms is used to alleviate the problem caused synchronization because it captures a full projection cycle, and the results are shown in Fig. 14. Fig. 14(a) shows one cross section of the phase error if the DBP method is used. The phase error appears to be random, which indicates that the phase error is not affected by the projector's nonlinear gamma. On the contrast, when the FSP method is used, the phase error is significantly large if there is no gamma correction, as shown in Fig. 14(b). This is because for the DBP method, only two intensity values (0 and 255) are used to produce the fringe images. However, for the FSP method, many intensity values are used, thus the nonlinear effect of the projector plays a vital role.

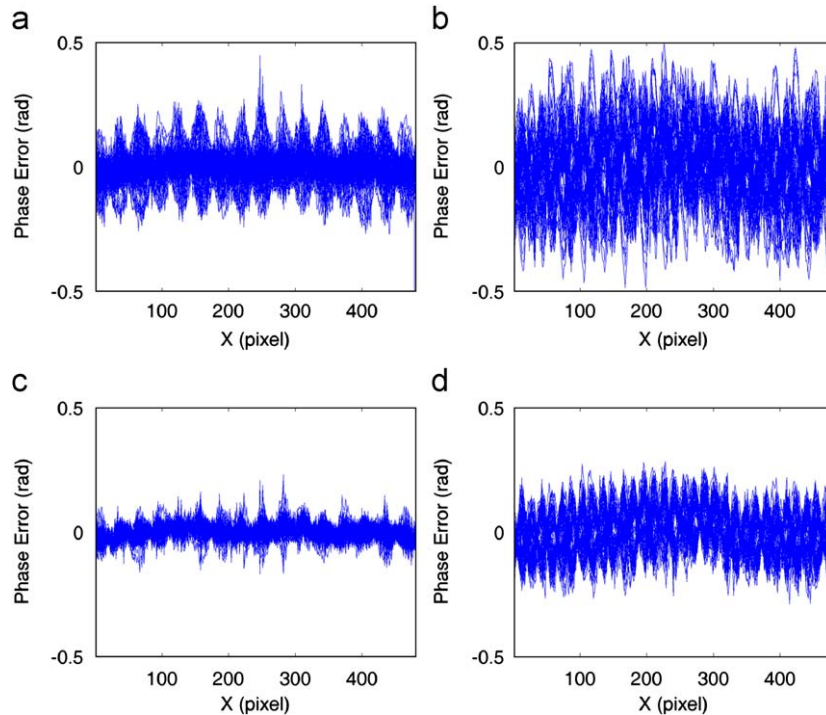


Fig. 12. Phase error for different exposure time when the camera and the projector is not synchronized. (a) The DBP method with exposure time of 3.33 ms (RMS error 0.060 rad); (b) the FSP method with exposure time of 3.33 ms (RMS error 0.136 rad); (c) the DBP method with exposure time of 6.67 ms (RMS error 0.029 rad); (d) the FSP method with exposure time of 6.67 ms (RMS error 0.084 rad).

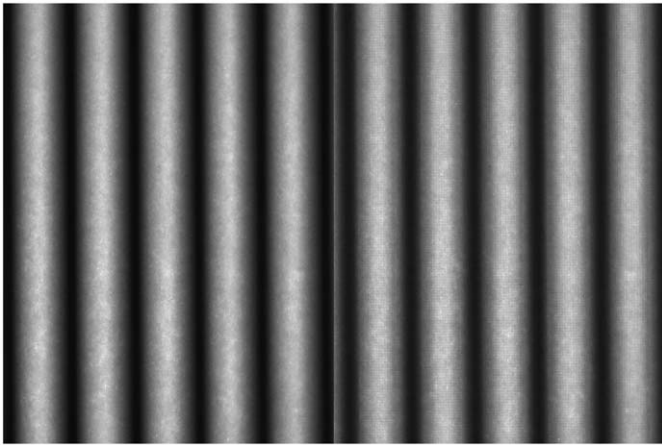


Fig. 13. The fringe image video captured over time for exposure time of 3.33 ms for DBP and FSP methods over time. The left half shows the DBP method, and the right half shows the FSP method.

5. Discussions

Comparing with the FSP approach, generating sinusoidal fringe patterns by the DBP method has the following major advantages:

- No precise synchronization between the projector and the camera is necessary. For the FSP method, more than two grayscale values are used, because the camera and the projector must be precisely synchronized for high-quality 3-D shape measurement. On the contrast, for the DBP method, the sinusoidal fringe patterns are generated by defocusing binary patterns, because the synchronization is less important.
- No gamma correction is required. The FSP method is very sensitive to the projector's nonlinear gamma effect, thus the gamma calibration is mandatory for a commercial digital video

projector. On the contrast, the DBP method is not sensitive to the projector gamma because only two grayscale levels are used.

However, comparing with FSP method, the DBP has the following major shortcomings:

- More difficult to achieve high accuracy. Because the sinusoidal patterns are not generated directly by the computer, the degree of defocusing affects the measurement. On the contrast, the FSP method uses an in-focused projector, it does not have this problem because the measuring objects are placed near its focal plane.
- Smaller measurement range. For the DBP method, the projector must be properly defocused to generate ideal sinusoidal fringe patterns, otherwise, the nonsinusoidal waveform will cause large error. On the contrast, the FSP method is not very sensitive to this problem because the degree of defocusing will not affect the fringe profile.

Nevertheless, comparing with its shortcomings, the DBP method can still be very useful when a commercial DLP projector is used for flexible 3-D shape measurement.

6. Conclusion

This paper has analyzed the phase errors caused by the following effects: (1) degree of defocusing, (2) exposure time, (3) synchronization, and (4) projector's nonlinear gamma. Both simulation and experiments showed that the degree of defocusing affects the phase error but within a large range of defocusing, the phase error is very small. Generating sinusoidal fringe images by defocusing the binary patterns are less sensitive to the exposure time used, the synchronization between the projector and the

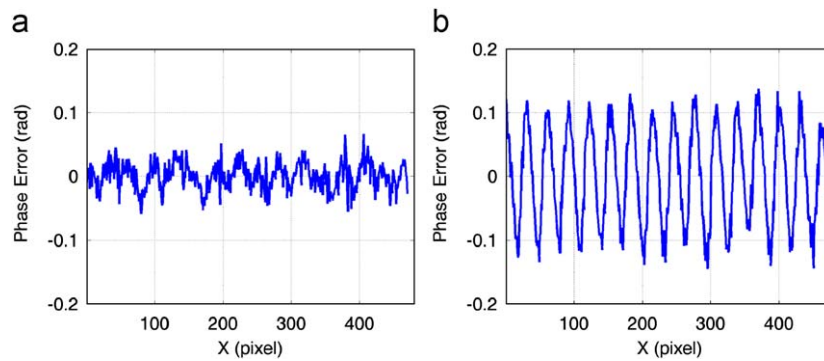


Fig. 14. Phase errors if no projector gamma correction is used. (a) DBP method (RMS error: 0.021 rad); (b) FSP method (RMS error: 0.077 rad).

camera, and the projector's nonlinear gamma. On the contrast, for a conventional method where the sinusoidal fringe images are generated by the computer and projected by the focused projector, all these factors must be controlled well to ensure high-quality measurement. In the meantime, the DBP method also has its shortcomings which related to controlling the profile to be ideal sinusoidal by proper defocusing.

References

- [1] Gorthi S, Rastogi P. Fringe projection techniques: whither we are?. *Opt Laser Eng* 2010;48:133–40.
- [2] Wang Z, Nguyen DA, Barnes JC. Some practical considerations in fringe projection Profilometry. *Opt Laser Eng* 2010;48:218–25.
- [3] Höfling R. High-speed 3D imaging by DMD technology. *Proc SPIE* 2004;5303:188–94.
- [4] Höfling R, Ahl E. ALP: universal DMD controller for metrology and testing. *Proc SPIE* 2004;5289:322–9.
- [5] Lei S, Zhang S. Flexible 3-D shape measurement method using projector defocusing. *Opt Lett* 2009;34(20):3080–2.
- [6] Hornbeck LJ. Digital light processing for high-brightness, high-resolution applications. *Proc SPIE* 1997;3013:27–40.
- [7] Takeda M, Mutoh K. Fourier transform profilometry for the automatic measurement of 3-D object shape. *Appl Opt* 1983;22:3977–82.
- [8] Guo H, Huang P. 3-D shape measurement by use of a modified Fourier transform method. *Proc SPIE* 2008;7066:70,660E.
- [9] Zhang S. Recent progresses on real-time 3-D shape measurement using digital fringe projection techniques. *Opt Laser Eng* 2010;40:149–58.
- [10] Schreiber H, Bruning JH. *Optical shop testing*, 3rd ed. Wiley; 2007. p. 547–666 [Chapter 14].
- [11] Ghiglia DC, Pritt MD. *Two-dimensional phase unwrapping: theory, algorithms, and software*. Wiley; 1998.
- [12] Ragulskies M, Aleksa A, Maskeliunas R. Contrast enhancement of time-averaged fringes based on moving average mapping functions. *Opt Laser Eng* 2009;47:768–73.
- [13] Hutchison DC. *Introducing BrilliantColor™ Technology*, Technical Report, Texas Instrument.
- [14] Huang PS, Zhang C, Chiang F-P. High-speed 3-D shape measurement based on digital fringe projection. *Opt Eng* 2002;42(1):163–8.
- [15] Kakunai S, Sakamoto T, Iwata K. Profile measurement taken with liquid-crystal grating. *Appl Opt* 1999;38(13):2824–8.
- [16] Zhang S, Huang PS. Phase error compensation for a three-dimensional shape measurement system based on the phase shifting method. *Opt Eng* 2007;46(6):063,601.
- [17] Zhang S, Yau S-T. Generic nonsinusoidal phase error correction for three-dimensional shape measurement using a digital video projector. *Appl Opt* 2007;46(1):36–43.
- [18] Guo H, He H, Chen M. Gamma correction for digital fringe projection profilometry. *Appl Opt* 2004;43:2906–14.
- [19] Pan B, Kemao Q, Huang L, Asundi A. Phase error analysis and compensation for nonsinusoidal waveforms in phase-shifting digital fringe projection profilometry. *Opt Lett* 2009;34(4):2906–14.